

# Machine Learning Based Molecular Index Modulation

Ozgur Kara<sup>\*</sup>, Gokberk Yaylali<sup>\*</sup>, Ali E. Pusane<sup>\*</sup>, *Senior Member, IEEE*, and Tuna Tugcu<sup>†</sup>, *Member, IEEE*

**Abstract**—As the promise of molecular communication via diffusion systems at nano-scale communication increases, designing molecular schemes robust to the inevitable effects of molecular interference has become of vital importance. We propose a novel approach of a CNN-based neural network architecture for a uniquely-designed molecular multiple-input-single-output topology in order to alleviate the damaging effects of molecular interference. In this study, we compare the performance of the proposed network with a naive-approach index modulation scheme and symbol-by-symbol maximum likelihood estimation with respect to bit error rate, and demonstrate that the proposed method yields better performance.

**Index Terms**—Molecular communications, multiple-input-single-output systems, index modulation, machine learning.

## I. INTRODUCTION

**M**OLECULAR communication is a novel communication technology that is inspired by nature. It enables information transmission via micro-machinery by exploiting several biologically-inspired methods. One of the basic approaches of molecular communication is molecular communication via diffusion (MCvD) [1]. It is based on the fact that the molecules in a fluid medium flow randomly through space, obeying the laws of Brownian motion. Messenger molecules are used to convey information between the transmitter (Tx) and the receiver (Rx) in a fashion in which the Tx releases molecules according to the encoded information, and the Rx counts the number of arriving molecules to decode the information. Since molecules propagate according to Brownian motion, they are subject to random propagation. Molecules that are delayed by more than the allotted signalling time are received in subsequent time slots and cause interference among information symbols. This is called inter-symbol interference (ISI) and is a major problem in MCvD systems.

Single-input-single-output (SISO) MCvD systems given in Fig. 1 are well-examined molecular communications systems, with their channel characteristics analytically derived in [2]. The literature presents a multitude of important contributions, including novel modulation methods and advanced reception methods to combat ISI [1], [3], [4]. Despite the many efforts proposed in the literature to reduce the degrading effects of ISI, communication performance—especially at high data rates—is usually lower bounded by a severe error floor. Therefore,

This work was supported in part by the Scientific and Technical Research Council of Turkey (TUBITAK) under Grant 119E190.

\* O. Kara, G. Yaylali, and A. E. Pusane are with the Department of Electrical and Electronics Engineering, Bogazici University, Istanbul, Turkey. (e-mail: {ozgur.kara, gokberk.yaylali, ali.pusane}@boun.edu.tr)

† T. Tugcu is with the Department of Computer Engineering, Bogazici University, Istanbul, Turkey. (e-mail: tugcu@boun.edu.tr)

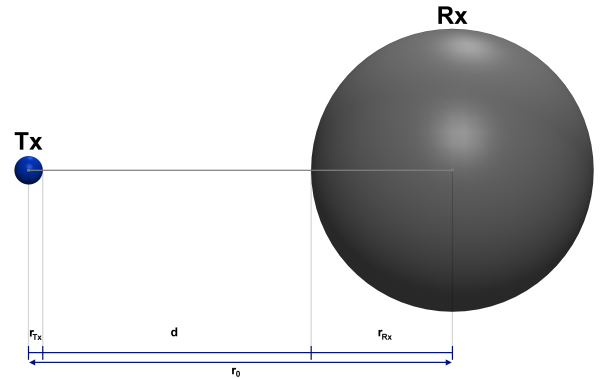


Fig. 1: Basic SISO communication scenario for MCvD.

multiple-input-multiple-output (MIMO) systems were introduced in [5].

Using multiple Tx/Rx is a conventional method in wireless communications to improve channel quality significantly. However, for ISI-affected applications, such as MCvD, it introduces the risk of further increasing the interference due to inter-link interference (ILI). One of the recently proposed MIMO techniques in MCvD is index modulation (IM) [6], which is adapted to molecular communications domain from wireless communications [7]. IM-based communication schemes are good candidates to employ multiple antennas in molecular communication due to their ability to combine the advantages of the spatial domain, while keeping the interference to a minimum. In index modulation, information is encoded into the selection of the Tx antenna unlike other modulation schemes. Rx detects which Tx antenna was used for transmission and decodes the information accordingly. This scheme enables us to reduce channel uses, which results in a cleaner channel with fewer stray molecules.

Employing additional transmitters/receivers always increases implementation complexity. Reducing this complexity while preserving the improved communication performance is one of the main goals in molecular MIMO applications. In order to reduce receiver complexity, a molecular multiple-input-single-output (MISO) topology is proposed in this paper. In contrast to the prevalent MIMO topologies, whose receiver regions are separated, MISO topology introduces compact receiver regions on the surface of a single central spherical receiver. Having a single receiver avoids the receiver complexity of molecular MIMO systems.

Receiver regions are located on the central spherical receiver and behave as perfect absorbing receiver surfaces.

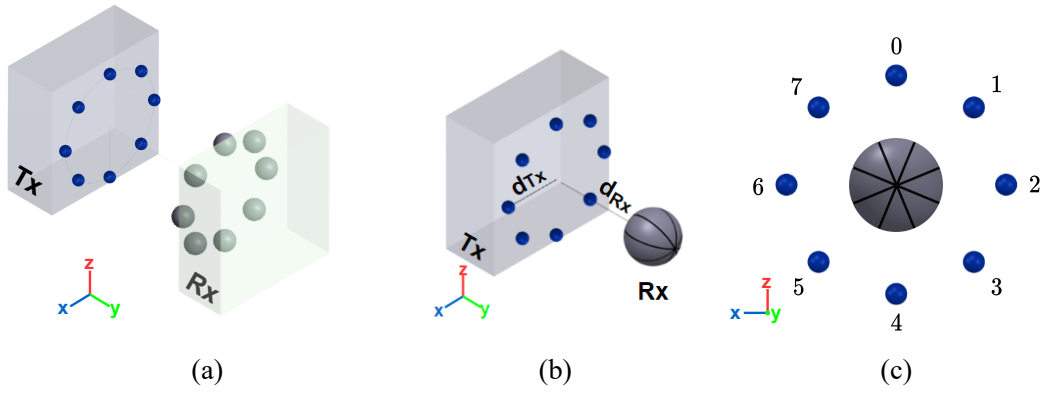


Fig. 2: Communication scenarios for  $n_{T_x} = 8$  (a) MIMO scenario (b) MISO scenario in 3D view (c) MISO scenario in 2D view. Black lines show the region boundaries on Rx and each region-transmitter conjugate is indexed from 0 to 7, consecutively.

As done in IM-based molecular MIMO modulations, each equi-areal receiver region corresponds to its conjugate Tx antenna. Suggested receiver topology is able to achieve the single Rx specifications, while mimicking the multi-receiver Rx designs with its distinctly separated receiver regions. This allows a new approach of molecular MISO topologies in molecular MIMO applications. Possible advantages of using such a single-receiver topology extend from designing systems with multiple single-antenna receivers coexisting in the same channel to creating robust modulation schemes for spatially erroneous topologies. The centralized receiver also allows the use of machine learning based detection algorithms, which are centralized to outperform conventional detection methods.

Organization of this paper is as follows: Section II demonstrates the proposed system topology. Furthermore, index modulation and ML-based detection process are briefly explained in this section. In Section III, network details and design specifications of machine-learning models are presented. Performances of the methods based on error rates are evaluated in Section IV. Finally, Section V concludes the paper.

## II. SYSTEM MODEL

### A. Topology

The considered MISO topology incorporates  $n_{T_x}$  distinct spherical transmitters with radius  $r_{T_x}$ , whose centers are placed onto a uniform circular array (UCA) with the ability to emit molecules into the diffusion channel, as well as a spherical receiver with radius  $r_{R_x}$  that is able to absorb the molecules arriving at its surface therewithal record their azimuth and elevation angles. Note that the receiver's center is perfectly placed onto the axis of the UCA with a distance of  $d_{R_x}$  from center. The closest distance between the center of the UCA and any of the transmitters is  $d_{T_x}$  (This topology is presented in Fig 2.b.). Additionally, the receiver sphere is partitioned into  $n_{T_x}$  different regions with the purpose that each region becomes a conjugate of oppositely positioned transmitter, and each Rx region-transmitter conjugate is indexed from 0 to  $(n_{T_x} - 1)$ , consecutively (Region boundaries are further shown in Fig 2.c.). For our experiments, the values are selected as follows:  $n_{T_x} = 8$ ,  $r_{T_x} = 0.5 \mu\text{m}$ ,  $r_{R_x} = 5 \mu\text{m}$ ,  $d_{R_x} = 15.5 \mu\text{m}$ ,  $d_{T_x} = 10 \mu\text{m}$ .

### B. Index Modulation

The first adaptations of molecular MIMO modulation into the molecular communication realm aimed to increase overall system throughput at a cost of worse error probabilities [6]. Using the channel multiple times during a symbol duration causes a significant amount of stray molecules –belonging to earlier channel uses– free-roaming in the channel, which results in heavy interference. To mitigate this effect, it is advantageous to use the channel only once per symbol duration. In this way, information is encoded into the *index* of the intended Tx antenna rather than any other aspect of the molecules, such as quantity [3], type [4], or temporal position [8]. The packet size of the encoded information depends on the number of antennas in use, i.e., for  $n_{T_x}$  antennas, information is encoded into  $\log_2(n_{T_x})$ -bit long packets. Rx antenna collects the messenger molecules through its receiver regions for a defined symbol duration, and detects the originating Tx antenna. Information is then extracted through the index of the detected Tx antenna. This general modulation scheme enables reliable information transmission with less channel use, which directly implies less interference. In the proposed topology case, receiver regions of Rx are compacted on the surface of the spherical centralized Rx. As aforementioned above, molecules absorbed by Rx are recorded with their azimuth and elevation angles, which enables Rx to perfectly detect which receiver region the molecules hit during a symbol period. Absorbed molecules are processed to decode the information.

### C. Propagation Model

The proposed machine-learning based approach utilizes the time series data of absorbed molecule rates recorded by  $n_{T_x}$  regions of the receiver at each time instant. To train the proposed model, the considered communication scenario is simulated in which the time series of  $n_{T_x}$  regions according to the number of molecules arrived are recorded after a randomly selected transmitter is allowed to emit  $M$  molecules at time  $t = (k - 1)t_s$ , where  $k \in \{1, 2, \dots, w\}$ ,  $t_s$  and  $w$  denote the symbol window time and window number, respectively. For our experiments,  $T = 5\text{s}$  is splitted into  $w \in \{3, 4, \dots, 10\}$  windows, each of which corresponds to a symbol time of  $t_s = \frac{T}{w}$ . In order to simulate random movement

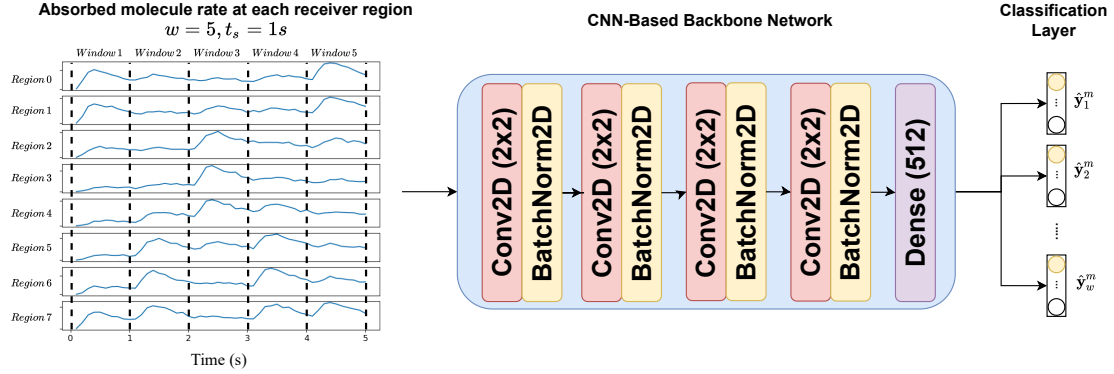


Fig. 3: Outline of the proposed model for  $w = 5$  and  $t_s = 5$  s. At each window following indexed transmitters emitted molecules: 0 – 6 – 3 – 6 – 0.

of the molecules in the driftless fluid environment, total time of communication scenarios is divided into steps of length  $\Delta t = 10^{-4}$  s in order to perform computer simulations and for each time interval  $[(k-1)t_s, kt_s)$ , molecules are emitted at instant time  $t = (k-1)t_s$ . The position of each molecule is updated in the 3D space according to

$$X(t + \Delta t) = X(t) + \Delta X, \quad (1)$$

$$Y(t + \Delta t) = Y(t) + \Delta Y, \quad (2)$$

$$Z(t + \Delta t) = Z(t) + \Delta Z, \quad (3)$$

where  $\Delta X$ ,  $\Delta Y$ , and  $\Delta Z$  are independent and identically distributed Gaussian random numbers with  $\mu = 0$  and  $\sigma^2 = 2D\Delta t$ , where the diffusion coefficient  $D$  is selected  $79.4 \mu\text{m}^2 \text{s}^{-1}$ . Furthermore, if a molecule hits the surface of the receiver, it is absorbed by the receiver and removed from the environment. Note that each receiver region records the number of absorbed molecules at every time instant,  $\Delta t = 10^{-4}$  s, which is then down-sampled to  $\Delta t = 10^{-1}$  s and normalized across regions in order to reduce computation complexity.

Intuitively, the naive approach, namely maximum count decoder (MCD), for predicting the correct transmitter for the  $k^{\text{th}}$  window for one sample  $m$  can be formulated as

$$\hat{y}_k^m = \arg \max_i \sum_{j=(k-1)t_s}^{kt_s} x_{i,j}^m, \quad (4)$$

where  $\mathbf{X}^m = (x_{i,j}^m)$ ,  $i = 1, \dots, n_{T_x}$ ,  $j = 1, \dots, \frac{T}{\Delta t}$ , i.e.,  $\mathbf{X}^m$  is the set of the time series for the  $m^{\text{th}}$  sample containing molecule rates of  $n_{T_x}$  regions for each discrete time and is row-wise summed over the interval of the  $k^{\text{th}}$  window. Thus, it can be found which region of the receiver is absorbing the maximum number of molecules, identical to the correct transmitter for the  $k^{\text{th}}$  window and the  $m^{\text{th}}$  sample denoted as  $\hat{y}_k^m$ , i.e.,  $\hat{\mathbf{y}}^m = (\hat{y}_k^m)$ ,  $k = 1, \dots, w$ .

### III. MACHINE LEARNING MODEL

Recent studies show that machine learning algorithms are capable of learning and benefiting from feature representations and are used in time series classification tasks. In particular, convolutional neural network based architectures have exhibited successful performance on these tasks even though they need to be fed with large amounts of data in the training phase.

For this reason, inspired by the works done by [9], [10], we prefer a CNN-based neural network model.

The task of detecting symbols at the receiver side turns into a multivariate time series classification problem. As each receiver region records the normalized rate of molecule distribution, the network is fed with  $n_{T_x} = 8$  different time series at once, each corresponding to the time series of the receiver region.

Each transmitter is indexed with a number from 0 to 7, consecutively (see Fig. 2-c). To predict the correct transmitter index for each window, a CNN-based neural network architecture is designed encompassing two main parts: the CNN-based model (given in Fig. 3) which is the backbone of the network, and a classifier layer that is specialized for each distinct window number  $w \in \{3, 4, \dots, 10\}$ . Based on the selection among eight of different windows, eight different models are implemented that are differentiated according to their number of *sub-heads* at the classifier layer. For each model, the classifier layer is separated into  $w$  *sub-heads*, each of which consists of eight neurons corresponding to the probability of having used the corresponding transmitter. In other words, the algorithm can be formulated as  $\mathcal{F}_w(\mathbf{X}^m | \mathbf{y}^m)$  where  $\mathbf{X}^m$  is a set of time series for  $m^{\text{th}}$  sample with dimensions  $(n_{T_x}, \frac{T}{\Delta t})$ ,  $\mathbf{y}^m$  is the one-hot encoded ground truth label with dimensions  $(w, n_{T_x})$ , and  $w$  is the window number. The objective of the machine learning model is to learn the relation between the molecule distribution over eight regions of the receiver and the *active* transmitter for each window. For each window number  $w$ , model training is done using the data generated with  $M = 10^5$  molecules, and each model is evaluated by the simulations done with varying molecule sizes  $M \in \{750, 1000, \dots, 3250\}$ .

The backbone network is composed of four convolutional layers with kernel sizes (2, 2) having 512 filters connected to a 512-dimensional dense layer after the convolutional layers. As an activation function, rectified linear unit (ReLU) is attached after each convolution block as well as dense layer. In order to alleviate the effects of over-fitting, batch normalization layer is utilized after each convolutional layer, which is beneficial in making neural networks faster and more stable by re-centering and scaling the mini-batches based on their mean and standard deviation values [11]. Softmax is applied after each *sub-head* in order to convert the linear outputs to a probability distribution. Particularly, the  $i^{\text{th}}$  element of the vector  $\hat{\mathbf{y}}_n^m, \hat{y}_{n,i}^m$ ,

denotes the probability of the  $i^{\text{th}}$  transmitter that is *active* for the  $n^{\text{th}}$  time window and  $m^{\text{th}}$  sample.

To train such a *multi-head* architecture for a classification task, categorical cross entropy loss function is applied through each of the *sub-heads*. To calculate the total model loss  $\mathcal{L}_{total}$  per mini-batch, all losses found for individual *sub-heads*, given as

$$\mathcal{L}_n(\hat{\mathbf{y}}_n, \mathbf{y}_n) = -\frac{1}{M} \sum_{m=1}^M \sum_{i=1}^{n_{Tx}} y_{n,i}^m \log(\hat{y}_{n,i}^m), \quad (5)$$

are averaged as

$$\mathcal{L}_{total} = \frac{1}{w} \sum_{n=1}^w \mathcal{L}_n(\hat{\mathbf{y}}_n, \mathbf{y}_n), \quad (6)$$

where  $\mathcal{L}_n(\hat{\mathbf{y}}_n, \mathbf{y}_n)$  is the calculated loss for the  $n^{\text{th}}$  *sub-head*,  $M$  is the mini-batch size,  $n_{Tx}$  denotes the number of transmitters (which always equals to 8 in our case), and  $\hat{y}_{n,i}^m$  and  $y_{n,i}^m$  denote the predicted value and one-hot encoded ground-truth label of the  $i^{\text{th}}$  neuron at the  $n^{\text{th}}$  window/*sub-head* for the  $m^{\text{th}}$  sample in the mini batch, respectively.

All models are trained with the stochastic gradient descent algorithm [12], using Adam [13] as an optimizer with a learning rate of 0.001, and the network is trained for 200 epochs with a batch size of 64. Hyper-parameter values are selected to be the best-performing ones based on hyper-parameter search experiments. In addition, using complicated models with more layers is not observed to significantly improve the performance, albeit their extra complexity.

#### IV. PERFORMANCE RESULTS

Communication performance of the suggested MISO topology in Section II-A is evaluated through Monte Carlo simulations. For performance evaluations, naive approach with Rx design of the maximum count decoder formulated in (4) is employed as the base modulation for comparisons. To compare the naive approach (Maximum Count Decoder, MCD) with an optimal Rx, symbol-by-symbol maximum-likelihood estimator (MLE) is also employed by considering the past  $L$  symbols to find the most likely symbol at each symbol duration. The unique contribution of this paper is the proposed machine learning model, and the required evaluations are conducted with the help of computer simulations as well. Communication simulations are conducted for both high and low data transmission rates. Also, a communication simulation with varying bit duration  $t_b$  is performed in order to show the convergence of performance under the ISI and ILI effects.

In Fig. 4, simulation results for high data transmission rate scenario are presented. Since the receiver regions are positioned adjacently as segments of spherical receiver, the probability of misreceived molecules is significantly high. This causes significant number of molecules to be absorbed adjacent receiver regions, resulting in ILI. For a high data transmission rate communication, ISI becomes the dominant interference problem for molecular realm along with ILI. MCD is prone to error due to significant interference. However, the symbol-by-symbol maximum-likelihood estimator shows the

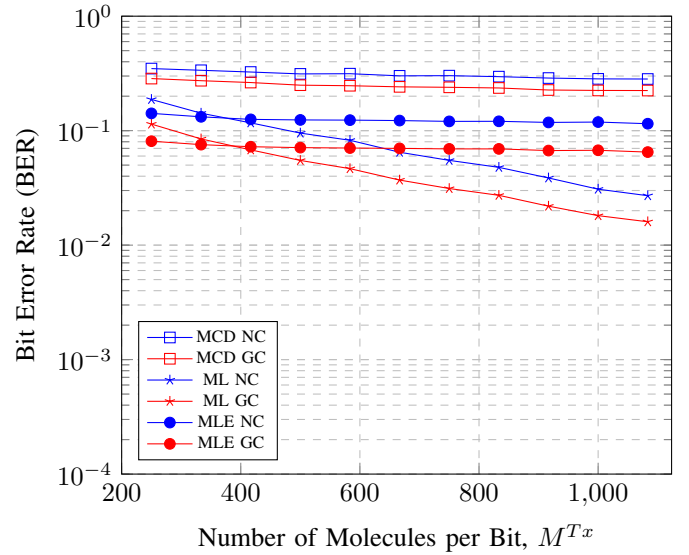


Fig. 4: Natural Coding (NC) and Gray Coding (GC) bit error rate for Maximum Count Decoder (MCD), Machine Learning (ML), Symbol-by-symbol Maximum Likelihood Estimation (MLE) approaches with  $t_b = 0.166$  s.

optimal performance MCD can reach. The proposed method shows strong communication performance compared to the optimal estimator in high data transmission rate scenario due to its ability to learn interference patterns with higher success than the optimal maximum-likelihood estimation.

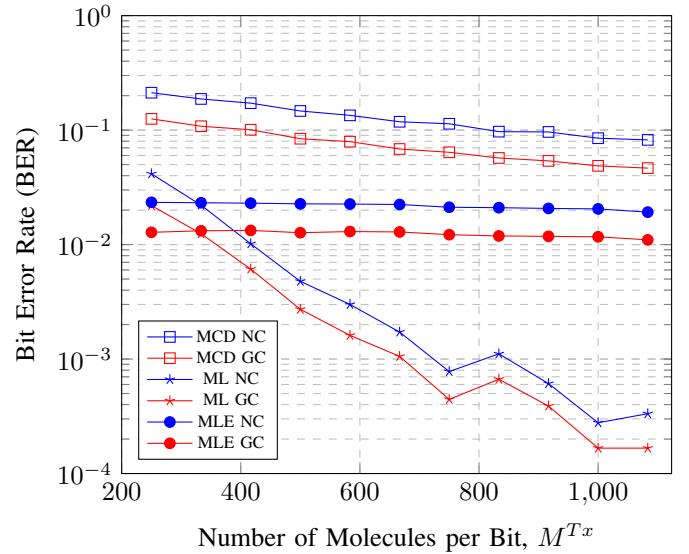


Fig. 5: Natural Coding (NC) and Gray Coding (GC) bit error rate for Maximum Count Decoder (MCD), Machine Learning (ML), Symbol-by-symbol Maximum Likelihood Estimation (MLE) approaches with  $t_b = 0.555$  s.

For low data transmission rate scenario given in Fig. 5, ILI becomes the dominant interference source. MCD is prone to errors due to considerable ILI. However, the proposed machine-learning method significantly dominates both MCD and the maximum-likelihood estimation in terms of bit error rate performance. The ability to learn and recognize interference patterns of our proposed method is enhanced when ISI loses power in low data transmission rates.

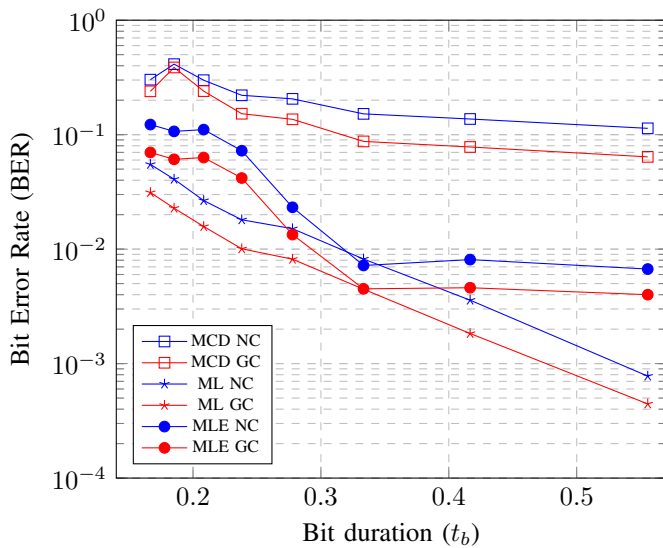


Fig. 6: Natural Coding (NC) and Gray Coding (GC) bit error rate for Maximum Count Decoder (MCD), Machine Learning (ML), Symbol-by-symbol Maximum Likelihood Estimation (MLE) approaches with varying  $t_b$  and 750 molecules per bit.

As explained before, the molecular MISO topology is vulnerable due to ILI, and it states why the betterment of this topology as  $t_b$  increases is limited. In the varying  $t_b$  scenario given in Fig. 6 where the number of molecules released per bit,  $M^{Tx}$ , is fixed, the topology shows its natural limits as, due to ILI, error performance improvement halts, resulting in an error floor. MCD has a significantly high error floor. On the other hand, the proposed machine-learning method continues to adapt under increasing  $t_b$  condition and shows no error-flooring. This strength comes from the natural ability of the proposed approach, which indicates continuous adaptation to learn patterns and recognize interference sequences. Nearly at all  $t_b$  scenarios, the proposed method outperforms both MCD and the optimal maximum-likelihood estimator.

## V. CONCLUSION AND FUTURE WORK

In this study, machine-learning based molecular index modulation scheme for a newly-proposed molecular MISO topology has been introduced. Said topology is new to the molecular communication realm, and enables to reduce receiver complexity drastically. Since the receiver regions are compacted on the single central receiver, implementation complexity of proposed scheme is realizable. It has been shown that the proposed molecular MISO topology is competent to provide adequate communication performance. Moreover, as aforementioned before, molecular MISO topology is able to fulfill the index modulation potential suggested by molecular MIMO topologies, which allows to conduct IM-based modulation schemes using molecular MISO topology without losing the improved communication performance superiority promised by index modulation. Presented results are able to show that said topology is performing satisfactory under basic IM-based modulation schemes, namely the naive-approach (MCD), for this paper.

Another unique contribution of this paper is the proposed machine-learning based molecular index modulation scheme. The adaptive nature of machine learning methods enables to overcome to communicative obstacles of molecular interference, namely ISI and ILI. It has been shown that ML-based modulation methods are prone to recognize interference patterns that are caused by the random nature of the molecular communication realm. The experimental results support the fact that the proposed ML-based modulation outperforms the native-approach of basic index modulation scheme conducted on molecular MISO topology, at both low and high data transmission rates. Due to our concerns for a fair comparison, a symbol-by-symbol maximum-likelihood estimation is performed. Based on the previous decisions and the channel characteristics knowledge, MLE detects the most likely antenna as the originating antenna for the considered symbol duration. The proposed machine-learning scheme outperforms the MLE at almost all symbol power levels, and has a much more promising betterment curve with respect to symbol power. Due to the nature of topology, molecular MISO topology is prone to suffer heavily from ILI. The proposed machine-learning method suggests an effective modulation scheme with significant ISI mitigation.

## REFERENCES

- [1] H. B. Yilmaz, N. R. Kim, and C. B. Chae, *Modulation Techniques for Molecular Communication via Diffusion*. Springer International Publishing, 2017, pp. 99–118.
- [2] H. B. Yilmaz, A. C. Heren, T. Tugcu, and C. B. Chae, “Three-dimensional channel characteristics for molecular communications with an absorbing receiver,” *IEEE Communications Letters*, vol. 18, no. 6, pp. 929–932, 2014.
- [3] M. H. Kabir, S. M. Riazul Islam, and K. S. Kwak, “D-MoSK modulation in molecular communications,” *IEEE Transactions on NanoBioscience*, vol. 14, no. 6, pp. 680–683, 2015.
- [4] M. S. Kuran, H. B. Yilmaz, T. Tugcu, and I. F. Akyildiz, “Modulation techniques for communication via diffusion in nanonetworks,” in *2011 IEEE International Conference on Communications (ICC)*, 2011, pp. 1–5.
- [5] B. Koo, C. Lee, H. B. Yilmaz, N. Farsad, A. Eckford, and C. Chae, “Molecular mimo: From theory to prototype,” *IEEE Journal on Selected Areas in Communications*, vol. 34, no. 3, pp. 600–614, 2016.
- [6] M. C. Gursoy, E. Basar, A. E. Pusane, and T. Tugcu, “Index modulation for molecular communication via diffusion systems,” *IEEE Transactions on Communications*, vol. 67, no. 5, pp. 3337–3350, 2019.
- [7] E. Basar, “Index modulation techniques for 5G wireless networks,” *IEEE Communications Magazine*, vol. 54, no. 7, pp. 168–175, 2016.
- [8] N. Garralda, I. Llatser, A. Cabellos-Aparicio, E. Alarcón, and M. Pierobon, “Diffusion-based physical channel identification in molecular nanonetworks,” *Nano Communication Networks*, vol. 2, pp. 196–204, 2011.
- [9] R. Assaf, I. Giurgiu, F. Bagehorn, and A. Schumann, “Mtex-cnn: Multivariate time series explanations for predictions with convolutional neural networks,” in *2019 IEEE International Conference on Data Mining (ICDM)*. IEEE, 2019, pp. 952–957.
- [10] C.-L. Liu, W.-H. Hsiao, and Y.-C. Tu, “Time series classification with multivariate convolutional neural network,” *IEEE Transactions on Industrial Electronics*, vol. 66, no. 6, pp. 4788–4797, 2018.
- [11] S. Ioffe and C. Szegedy, “Batch normalization: Accelerating deep network training by reducing internal covariate shift,” in *International conference on machine learning*. PMLR, 2015, pp. 448–456.
- [12] H. Robbins and S. Monro, “A stochastic approximation method,” *The annals of mathematical statistics*, pp. 400–407, 1951.
- [13] D. P. Kingma and J. Ba, “Adam: A method for stochastic optimization,” *arXiv preprint arXiv:1412.6980*, 2014.